Gravitational wave signatures of lepton universality violation

Bartosz Fornal

Department of Physics and Astronomy, University of Utah, Salt Lake City, Utah 84112, USA

(Received 24 June 2020; accepted 1 December 2020; published 15 January 2021)

We analyze the prospects for using gravitational waves produced in early universe phase transitions as a complementary probe of the flavor anomalies in B meson decays. We focus on the left-right SU(4) model, for which the strength of the observed lepton universality violation and consistency with other experiments impose a vast hierarchy between the symmetry breaking scales. This leads to a multipeaked gravitational wave signature within the reach of upcoming gravitational wave detectors.

DOI: 10.1103/PhysRevD.103.015018

I. INTRODUCTION

Although the Standard Model (SM) does not provide all the answers to fundamental questions in particle physics and needs to be augmented by new physics, nearing half a century since its formulation [1–5] it has certainly stood the test of time with respect to its predictive power. A huge number of models beyond the SM have been constructed proposing solutions to the outstanding problems; however, it is not certain which of them, if any, is realized in nature. At this time, guidance from experiment is especially important in order to achieve further progress on the theory side.

So far, among the strongest experimental hints of new physics are the indications of lepton universality violation in B meson decays, the so-called $R_{K^{(*)}}$ and $R_{D^{(*)}}$ anomalies. Although the $R_{D^{(*)}}$ anomalies (reported by *BABAR* [6], Belle [7], and LHCb [8]) have not been confirmed in the most recent set of Belle data [9], and the R_{K^*} anomaly reported by LHCb [10] has become less significant [11], the R_K anomaly [12] has persisted with new LHCb data [13].

From an effective theory point of view [14–22] the observed signals of lepton universality violation are best accounted for by either the vector leptoquark $(3,1)_{\frac{2}{3}}$ or $(3,3)_{\frac{2}{3}}$. A natural origin of the former in the context of flavor anomalies has been proposed in [23], where it was suggested that this leptoquark can be the gauge boson of a Pati-Salam-type unified model. This has been followed by several efforts aimed at explaining either both the $R_{K^{(*)}}$ and $R_{D^{(*)}}$ anomalies [24–33] or just the $R_{K^{(*)}}$ [34,35] through the vector leptoquark $(3,1)_{\frac{2}{3}}$ in UV complete models. Other explanations of the anomalies include Z' bosons [36–41] and scalar leptoquarks [42–45].

Since the latest results on $R_{D^{(*)}}$ from Belle [9] are consistent with the SM, lowering the overall significance of those anomalies, in this paper we focus on the solution to just the $R_{K^{(*)}}$ anomalies offered by the *left-right SU(4) model* [35]. This is the only model for the flavor anomalies proposed so far which does not require any mixing between quarks and new vectorlike fermions. Apart from the existing experimental searches for lepton universality violation, the only other conventional way of looking for signatures of this model is to produce the vector leptoquark in particle colliders. However, given its large mass of ∼10 TeV, this would require using the 100 TeV Future Circular Collider, whose construction has not yet been approved.

A new window of opportunities for probing particle physics models has recently been opened by gravitational wave experiments. The gravitational wave detectors LIGO [46] and Virgo [47], in addition to observing signals from astrophysical phenomena such as black hole and neutron star mergers, have unique capabilities of detecting the imprints of cosmic events in the early universe, providing access to regions of parameter space unexplored so far in various extensions of the SM. This will be even more promising with future experiments such as the Laser Interferometer Space Antenna (LISA) [48], Cosmic Explorer (CE) [49], Einstein Telescope (ET) [50], DECIGO [51], or Big Bang Observer (BBO) [52].

One class of particle physics signals that gravitational wave detectors are sensitive to arises from early universe phase transitions. If the scalar potential has a nontrivial vacuum structure, the universe could have settled in a state which, as the temperature dropped, became metastable. The universe would then undergo a transition via thermal fluctuations from the false vacuum to the true vacuum. During such a first order phase transition, bubbles of true vacuum would form in different patches of the universe and

start expanding. Gravitational waves would be generated from bubble wall collisions, magnetohydrodynamic turbulence, and sound shock waves of the early universe plasma generated by the bubble's violent expansion. At the Lagrangian level of a theory, a phase transition is triggered by spontaneous symmetry breaking. In models with a rich gauge structure, multiple steps of symmetry breaking can occur, resulting in a chain of phase transitions, each generating gravitational waves.

First order phase transitions from symmetry breaking have been studied with respect to their predictions regarding the gravitational wave signals in various models of new physics (see, e.g., [53–73]). Here we investigate the complementarity between gravitational wave experiments and direct searches for lepton universality violation. Such a connection has recently been made in [70] in the context of the Pati-Salam cubed model [26], which consists of three copies of the Pati-Salam gauge group, each for a different family of particles. In the left-right SU(4) model which we are considering, the gauge group is common to all the families. The symmetry breaking pattern consists of three steps, each leading to a distinct peak in the gravitational wave spectrum. The position of the two lower-frequency peaks in the three-peaked gravitational wave spectrum is determined by the magnitude of the flavor anomalies, offering a way to discriminate the model.

II. LEFT-RIGHT SU(4) MODEL

In this section we provide a summary of the most important properties of the model (for further details, see [35]).

The model is based on the gauge group

$$\mathcal{G} = \mathrm{SU}(4)_L \times \mathrm{SU}(4)_R \times \mathrm{SU}(2)_L \times \mathrm{U}(1)'. \tag{1}$$

The fermion, scalar, and vector particle contents are provided in Table I. The gauge group $\mathcal{G}$ is broken by the vacuum expectation values (VEVs) of the scalar fields $\hat{\Sigma}_R$, $\hat{\Sigma}_L$, and $\hat{\Sigma}$. The parameters of the scalar potential can be chosen such that the following VEV structure is obtained,

$$\langle \hat{\Sigma}_R^i \rangle = \frac{v_R}{\sqrt{2}}\delta^{i4}, \qquad \langle \hat{\Sigma}_L^i \rangle = \frac{v_L}{\sqrt{2}}\delta^{i4},$$
$$\langle \hat{\Sigma} \rangle = \frac{v_\Sigma}{\sqrt{2}}\mathrm{diag}(1,1,1,z), \tag{2}$$

where $z > 0$. The $\mathrm{SU}(4)_R$ symmetry is broken at a high scale v_R in order to suppress right-handed lepton flavor changing currents and comply with the stringent experimental bounds, whereas the other scales, v_L and v_Σ, are constrained by the size of the $R_{K^{(*)}}$ anomalies to be much lower than v_R. We make an additional assumption that there is also a hierarchy between the scales v_L and v_Σ, i.e.,

$$v_R \gg v_L \gg v_\Sigma. \tag{3}$$

This implies the following symmetry breaking pattern (with the numerical choice for the VEVs explained below):

$$\begin{aligned}
&\mathrm{SU}(4)_L \times \mathrm{SU}(4)_R \times \mathrm{SU}(2)_L \times \mathrm{U}(1)' \\
&\qquad\downarrow \quad v_R \sim 5000\ \mathrm{TeV} \\
&\mathrm{SU}(4)_L \times \mathrm{SU}(3)_R \times \mathrm{SU}(2)_L \times \mathrm{U}(1)'' \\
&\qquad\downarrow \quad v_L \sim 40\ \mathrm{TeV} \\
&\mathrm{SU}(3)_L \times \mathrm{SU}(3)_R \times \mathrm{SU}(2)_L \times \mathrm{U}(1)_Y \\
&\qquad\downarrow \quad v_\Sigma \sim 7\ \mathrm{TeV} \\
&\mathrm{SU}(3)_c \times \mathrm{SU}(2)_L \times \mathrm{U}(1)_Y.
\end{aligned}$$

The $\mathrm{U}(1)'$ charge Y', the $\mathrm{U}(1)''$ charge Y'', and the SM hypercharge Y are related via

$$Y'' = Y' + \frac{1}{6}\mathrm{diag}(1,1,1,-3),$$
$$Y = Y'' + \frac{1}{6}\mathrm{diag}(1,1,1,-3). \tag{4}$$

The covariant derivative can be written as

$$D_\mu = \partial_\mu + ig_L G^A_{L\mu} T^A_L + ig_R G^A_{R\mu} T^A_R + ig_2 W^a_\mu T^a + ig'_1 Y'_\mu Y', \tag{5}$$

where the index $A = 1, \ldots, 15$, the index $a = 1, 2, 3$, and T^A_L, T^A_R, T^a, Y' are the $\mathrm{SU}(4)_L$, $\mathrm{SU}(4)_R$, $\mathrm{SU}(2)_L$, $\mathrm{U}(1)'$ generators, respectively. At the low scale, the gauge couplings g_L, g_R, g'_1 are related to the SM gauge couplings g_s, g_1 via

$$g_s = \frac{g_L g_R}{\sqrt{g_L^2 + g_R^2}}, \quad g_1 = \frac{g'_1 g_L g_R}{\sqrt{\frac{2}{3}g'^2_1(g_L^2 + g_R^2) + g_L^2 g_R^2}}. \tag{6}$$

The Lagrangian terms describing the fermion masses are

$$\mathcal{L}_f = [y^d_{ij}\overline{\hat{\Psi}^i_L}\hat{H}_d\hat{\Psi}^{dj}_R + y^u_{ij}\overline{\hat{\Psi}^i_L}\hat{H}_u\hat{\Psi}^{uj}_R + Y_{ij}\overline{\hat{\chi}^i_L}\hat{\Sigma}\hat{\chi}^j_R] + \mathrm{H.c.} + y^{u\prime}_{ij}\overline{(\hat{\Psi}^{ui}_R)^c}\hat{\Phi}_{10}\hat{\Psi}^{uj}_R, \tag{7}$$

where the scalar field $\hat{\Phi}_{10} = (1, \overline{10}, 1, -1)$ develops a high-scale VEV $v_{10} \sim 10^{13}$ GeV and provides a seesaw mechanism for the neutrino masses, $m_\nu \sim v^2/v_{10}$ with v being the SM Higgs VEV. After symmetry breaking down to the SM gauge group, the fermion mass terms become

TABLE I. The fermion, scalar, and vector particle content of the model. The masses were calculated assuming the hierarchical VEV structure $v_{10} \gg M \gg v_R \gg v_L \gg v_\Sigma$.

Fermion fields		
$\mathcal{G}$	SM representation	Masses
$\hat{\Psi}_L = (4,1,2,0)$	$Q_L = (3,2)_{\frac{1}{6}}$ $L_L = (1,2)_{-\frac{1}{2}}$	SM masses for quarks and leptons $m_\nu \sim \frac{v^2}{v_{10}}$ $M_{\nu_R} \sim v_{10}$
$\hat{\Psi}^d_R = (1,4,1,-\frac{1}{2})$	$d_R = (3,1)_{-\frac{1}{3}}$ $e_R = (1,1)_{-1}$	
$\hat{\Psi}^u_R = (1,4,1,\frac{1}{2})$	$u_R = (3,1)_{\frac{2}{3}}$ $\nu_R = (1,1)_0$	
$\hat{\chi}_L = (\bar{4},1,2,0)$	$Q'_L = (\bar{3},2)_{-\frac{1}{6}}$ $L'_L = (1,2)_{\frac{1}{2}}$	$(M_{Q'})_{ij} = \frac{Y_{ij}}{\sqrt{2}} v_\Sigma$ $(M_{L'})_{ij} = \frac{Y_{ij}}{\sqrt{2}} z v_\Sigma$
$\hat{\chi}_R = (1,\bar{4},2,0)$	$Q'_R = (\bar{3},2)_{-\frac{1}{6}}$ $L'_R = (1,2)_{\frac{1}{2}}$	

Scalar fields		
$\mathcal{G}$	SM representation	Masses
$\hat{\Sigma}_R = (1,4,1,\frac{1}{2})$	$(3,1)_{\frac{2}{3}}$, $(1,1)_0$	Radial mode: $\sqrt{2\lambda_R} v_R$
$\hat{\Sigma}_L = (4,1,1,\frac{1}{2})$	$(3,1)_{\frac{2}{3}}$, $(1,1)_0$	Radial mode: $\sqrt{2\lambda_L} v_L$
$\hat{\Sigma} = (\bar{4},4,1,0)$	$(8,1)_0$, $(3,1)_{\frac{2}{3}}$, $(1,1)_0$, $(\bar{3},1)_{-\frac{2}{3}}$, $(1,1)_0$	Radial modes $\sim\sqrt{\lambda^{(\prime)}_\Sigma} v_\Sigma$
$\hat{H}_d = (4,\bar{4},2,\frac{1}{2})$	$(8,2)_{\frac{1}{2}}$, $(3,2)_{\frac{7}{6}}$, $(1,2)_{\frac{1}{2}}$, $(\bar{3},2)_{-\frac{1}{6}}$, $(1,2)_{\frac{1}{2}}$	$\sim M$, $m_{S'_1} = m_h$
$\hat{H}_u = (4,\bar{4},2,-\frac{1}{2})$	$(8,2)_{-\frac{1}{2}}$, $(3,2)_{\frac{1}{6}}$, $(1,2)_{-\frac{1}{2}}$, $(\bar{3},2)_{-\frac{7}{6}}$, $(1,2)_{-\frac{1}{2}}$	$\sim M$
$\hat{\Phi}_{10} = (1,\overline{10},1,-1)$	$(\bar{6},1)_{-\frac{4}{3}}$, $(\bar{3},1)_{-\frac{2}{3}}$, $(1,1)_0$	$\sim v_{10}$

Vector fields		
$\mathcal{G}$	SM representation	Masses
	g, W^a_μ, Z	SM particles
$G^A_{R\mu}$	$X_R = (3,1)_{\frac{2}{3}}$ $X^\dagger_R = (\bar{3},1)_{-\frac{2}{3}}$	$M_{X_R} = \frac{1}{2} g_R v_R$
Z'_μ	$Z'_R = (1,1)_0$	$M_{Z'_R} = \frac{1}{2}\sqrt{g'^2_1 + \frac{3}{2} g^2_R} v_R$
$G^A_{L\mu}$	$X_L = (3,1)_{\frac{2}{3}}$ $X^\dagger_L = (\bar{3},1)_{-\frac{2}{3}}$	$M_{X_L} = \frac{1}{2} g_L v_L$
W^a_μ	$Z'_L = (1,1)_0$ $G' = (8,1)_0$	$M_{Z'_L} = \sqrt{\frac{3g'^2_1(g^2_L+g^2_R)+\frac{9}{2}g'^2_1 g^2_R}{8(g'^2_1+\frac{3}{2}g^2_R)}} v_L$ $M_{G'} = \frac{1}{\sqrt{2}}\sqrt{g^2_L + g^2_R} v_\Sigma$

$$\mathcal{L}_f \supset \Big[y^d_{ij} \overline{L^i_L} S_1 e^j_R + y^d_{ij} \overline{Q^i_L} S_2 d^j_R + y^u_{ij} \overline{L^i_L} S^*_3 \nu^j_R + y^u_{ij} \overline{Q^i_L} S^*_4 u^j_R + \frac{1}{\sqrt{2}} Y_{ij} v_\Sigma (\overline{Q'^i_L} Q'^j_R + z \overline{L'^i_L} L'^j_R) \Big] + \text{H.c.} + y^{u\prime}_{ij} v_{10} \overline{(\nu^i_R)^c} \nu^j_R. \tag{8}$$

The scalar sector is described by the Lagrangian

$$\mathcal{L}_s = |D_\mu \hat{\Sigma}_R|^2 + |D_\mu \hat{\Sigma}_L|^2 + |D_\mu \hat{\Sigma}|^2 + |D_\mu \hat{H}_d|^2 + |D_\mu \hat{H}_u|^2 + |D_\mu \hat{\Phi}_{10}|^2 + V(\hat{\Sigma}_R, \hat{\Sigma}_L, \hat{\Sigma}, \hat{H}_d, \hat{H}_u, \hat{\Phi}_{10}), \tag{9}$$

where the scalar potential contains the following terms (traces are implicit):

$$\begin{aligned} V \supset & -\mu_R^2|\hat{\Sigma}_R|^2 + \lambda_R|\hat{\Sigma}_R|^4 - \mu_L^2|\hat{\Sigma}_L|^2 + \lambda_L|\hat{\Sigma}_L|^4 \\ & - \mu_\Sigma^2|\hat{\Sigma}|^2 + \lambda_\Sigma(\hat{\Sigma}\hat{\Sigma}^\dagger)^2 + \lambda'_\Sigma|\hat{\Sigma}\hat{\Sigma}^\dagger|^2 \\ & + \lambda_{12}|\hat{\Sigma}_L|^2|\hat{\Sigma}_R|^2 + \lambda_{13}|\hat{\Sigma}_L|^2|\hat{\Sigma}|^2 + \lambda_{23}|\hat{\Sigma}_R|^2|\hat{\Sigma}|^2 \\ & + \lambda'_{13}|\hat{\Sigma}_L\hat{\Sigma}|^2 + \lambda'_{23}|\hat{\Sigma}_R^\dagger\hat{\Sigma}|^2 + [\kappa\hat{\Sigma}_L\hat{\Sigma}\hat{\Sigma}_R^\dagger + \text{H.c.}] \\ & + M_u^2|\hat{H}_u|^2 + M_d^2|\hat{H}_d|^2. \end{aligned} \tag{10}$$

In Eq. (10) we left out the cross terms between $\hat{\Sigma}_R$, $\hat{\Sigma}_L$, $\hat{\Sigma}$ and $\hat{H}_u$, $\hat{H}_d$; the full form of the scalar potential is given in [35].

As discussed in [35], it is possible to tune the parameters of the scalar potential such that only one linear combination of the fields S_1, S_2, S_3, S_4 is light, reproducing the SM scalar sector at low energies ($S'_1 \equiv H$). The remaining fields $S'_{2,3,4}$ and all other components of $\hat{H}_u$ and $\hat{H}_d$ have masses set by the hard mass parameters M_u, M_d, which we take to be $M_u = M_d \equiv M \gg v_R$. The relative mass hierarchies between the SM down-type quarks and charged leptons are reproduced reasonably well within this minimal setup. One can also introduce into the model the scalar representation $\hat{\Phi}_{15} = (15, 1, 1, 0)$ that develops a VEV at a high scale and leads to terms $\overline{\hat{\Psi}_L^i}\hat{H}_d\hat{\Psi}_R^{dj}\hat{\Phi}_{15}/\Lambda$ providing distinct contributions to the quark and lepton masses.

The Lagrangian terms involving the fermion and vector fields are given by

$$\begin{aligned} \mathcal{L}_v = & \overline{\hat{\Psi}}_L i\not{D}\hat{\Psi}_L + \overline{\hat{\Psi}}^u_R i\not{D}\hat{\Psi}^u_R + \overline{\hat{\Psi}}^d_R i\not{D}\hat{\Psi}^d_R \\ & + \bar{\hat{\chi}}_R i\not{D}\hat{\chi}_R + \bar{\hat{\chi}}_L i\not{D}\hat{\chi}_L, \end{aligned} \tag{11}$$

which, at the low scale, result in the following interactions between quarks, leptons, and gauge leptoquarks:

$$\begin{aligned} \mathcal{L}_v \supset & \frac{g_L}{\sqrt{2}} X_{L\mu}[L^u_{ij}(\bar{u}^i\gamma^\mu P_L\nu^j) + L^d_{ij}(\bar{d}^i\gamma^\mu P_L e^j)] \\ & + \frac{g_R}{\sqrt{2}} X_{R\mu}[R^u_{ij}(\bar{u}^i\gamma^\mu P_R\nu^j) + R^d_{ij}(\bar{d}^i\gamma^\mu P_R e^j)] + \text{H.c.}, \end{aligned} \tag{12}$$

where L^u, L^d, R^u, and R^d are mixing matrices. They are all unitary and related to the Cabibbo-Kobayashi-Maskawa matrix and the Pontecorvo-Maki-Nakagawa-Sakata matrix via $L^u = V_{\text{CKM}}L^d U_{\text{PMNS}}$ and $R^u = V_{\text{CKM}}R^d U_{\text{PMNS}}$.

To circumvent the stringent experimental constraints on lepton universality violation [74–94], the scale of $\text{SU}(4)_R$ breaking needs to be $v_R \gtrsim 5000$ TeV for a generic unitary matrix R^d [35]. At the same time, in order for the vector leptoquark X_L to explain the $R_{K^{(*)}}$ anomalies, one requires [35]

$$\frac{M_{X_L}}{g_L\sqrt{\text{Re}(L^d_{22}L^{d*}_{32} - L^d_{21}L^{d*}_{31})}} \approx 23 \text{ TeV}. \tag{13}$$

Because of the unitarity of the matrix L^d, this relation can be fulfilled only if $M_{X_L} \lesssim (23 \text{ TeV})g_L$. The experimental constraints then force L^d to be of the form

$$L^d \approx e^{i\phi}\begin{pmatrix} \delta_1 & \delta_2 & 1 \\ e^{i\phi_1}\cos\theta & e^{i\phi_2}\sin\theta & \delta_3 \\ -e^{-i\phi_2}\sin\theta & e^{-i\phi_1}\cos\theta & \delta_4 \end{pmatrix}, \tag{14}$$

where $\delta_i \lesssim 0.02$. The allowed leptoquark mass in Eq. (13) is maximized for $\theta = \pi/4$ and $\phi_1 + \phi_2 = 0$, which implies

$$v_L \lesssim 46 \text{ TeV}. \tag{15}$$

Given the assumption $v_L \gg v_\Sigma$, the lower bound on v_Σ is of relevance. It arises from LHC dijet searches for colorons [95] and translates to $v_\Sigma > 6.6$ TeV. We take $v_\Sigma = 7$ TeV. The only particles other than G' with masses governed by v_Σ are the radial modes of $\hat{\Sigma}$ and the vectorlike fermions Q' and L'. The former do not couple to SM quarks, and our choice $v_\Sigma = 7$ TeV is consistent with experimental bounds, even for $\lambda_\Sigma^{(\prime)}$ as small as $\sim 3 \times 10^{-3}$. The latter do not mix with SM quarks, so for $Y_{ij} \sim 1$ this choice of v_Σ is also consistent with collider searches, even for a relatively small z.

In the subsequent analysis, we consider the hierarchical symmetry breaking pattern with the following VEVs:

$$v_R \approx 5000 \text{ TeV}, \quad v_L \approx 40 \text{ TeV}, \quad v_\Sigma \approx 7 \text{ TeV}. \tag{16}$$

The VEV structure in Eq. (2) can be realized if the parameters of the scalar potential satisfy the conditions: $\lambda'_{13} > 4\lambda_\Sigma(v_\Sigma/v_L)^2$, $\lambda'_{23} > 4\lambda_\Sigma(v_\Sigma/v_R)^2$, $\lambda_\Sigma^{(\prime)} > 0$, and $\kappa < 0$. We also note that the hierarchy between the VEVs in Eq. (16) is not protected against radiative corrections and requires a tuning of the parameters λ_{12}, λ_{13}, and λ_{23}.

III. EFFECTIVE POTENTIAL

Because of the vast hierarchy of scales in the model and small cross terms in the scalar potential, the three steps of symmetry breaking can be considered independently from one another. Denoting the background fields as

$$\begin{aligned} & \phi_R \equiv \text{Re}(\hat{\Sigma}_R)_4\sqrt{2}, \qquad \phi_L \equiv \text{Re}(\hat{\Sigma}_L)_4\sqrt{2}, \\ & \phi_\Sigma \equiv \text{Re}(\hat{\Sigma})^1_1\sqrt{2}, \end{aligned} \tag{17}$$

the effective potential splits into three pieces,

$$V_{\text{eff}} = V^{(R)}_{\text{eff}}(\phi_R) + V^{(L)}_{\text{eff}}(\phi_L) + V^{(\Sigma)}_{\text{eff}}(\phi_\Sigma). \tag{18}$$

Before analyzing the phase transitions, we first discuss the effective potential in the general case. We adopt the collective notation for the background fields $\phi = \phi_R, \phi_L, \phi_\Sigma$; the VEVs $v = v_R, v_L, v_\Sigma$; and the quartic couplings $\lambda = \lambda_R, \lambda_L, \lambda_\Sigma, \lambda'_\Sigma$. Each piece of the effective potential consists of a tree-level part, a one-loop Coleman-Weinberg correction, and a finite temperature contribution,

$$V_{\rm eff}(\phi, T) = V_{\rm tree}(\phi) + V_{\rm loop}(\phi) + V_{\rm temp}(\phi, T). \quad (19)$$

Using the fact that the minimum of the tree-level potential for $\phi = \phi_R, \phi_L$ is at $v = \mu/\sqrt{\lambda}$, one can write

$$V_{\rm tree}(\phi) = -\frac{1}{2}\lambda v^2 \phi^2 + \frac{1}{4}\lambda \phi^4. \quad (20)$$

The tree-level potential for $\phi = \phi_\Sigma$ contains terms involving λ_Σ and λ'_Σ with different z dependences.

To obtain the Coleman-Weinberg term, we implement the cutoff regularization scheme and assume that the minimum of the one-loop potential and the mass of ϕ are the same as their tree-level values [96]. In this scheme, the one-loop zero temperature correction is

$$V_{\rm loop}(\phi) = \sum_{\rm particles} \frac{n_i}{64\pi^2}\left\{ m_i^4(\phi)\left[\log\left(\frac{m_i^2(\phi)}{m_i^2(v)}\right) - \frac{3}{2}\right] + 2m_i^2(\phi) m_i^2(v)\right\}, \quad (21)$$

where the sum is over all particles charged under the gauge group that undergoes symmetry breaking, including the Goldstone bosons $\chi_{\rm GB}$, n_i is the number of degrees of freedom with an extra minus sign for fermions, and $m_i(\phi)$ are the background field-dependent masses. For the contribution of the Goldstone bosons one needs to replace $m_{\chi_{\rm GB}}(v) \to m_\Phi(v)$, where Φ is the radial mode.

The temperature-dependent part of the potential consists of the one-loop finite temperature contribution $V^{(1)}_{\rm temp}(\phi, T)$ and, in case of bosonic degrees of freedom, the Daisy diagrams contribution $V^{(2)}_{\rm temp}(\phi, T)$. The corresponding formulas are given by [97]

$$V^{(1)}_{\rm temp}(\phi, T) = \frac{T^4}{2\pi^2}\sum_{\rm particles} n_i \int_0^\infty dy y^2 \times \log\left(1 \mp e^{-\sqrt{m_i^2(\phi)/T^2 + y^2}}\right), \quad (22)$$

where the minus sign is for bosons and the plus sign is for fermions, and

$$V^{(2)}_{\rm temp}(\phi, T) = \frac{T}{12\pi}\sum_{\rm bosons} n'_i\{m_i^3(\phi) - [m_i^2(\phi) + \Pi_i(T)]^{\frac{3}{2}}\}. \quad (23)$$

The thermal masses $\Pi_i(T)$ can be calculated following the prescription provided in [98].

IV. PHASE TRANSITIONS

A strong first order phase transition is required to produce a gravitational wave signal. This occurs when the effective potential develops a barrier separating the false vacuum from the true vacuum. We perform a scan over the parameters of the model and identify the regions of parameter space which yield gravitational wave signals most promising for detection. As a benchmark scenario, we adopt the values $\lambda_R(v_R) = 0.011$, $\lambda_L(v_L) = 0.029$, and $\lambda^{(\prime)}_\Sigma(v_\Sigma) = 0.036$, as this choice of parameters leads to a strong gravitational wave signal. For such small quartics the only relevant contributions to the field-dependent masses and thermal masses are those involving the gauge couplings $g_{R/L}$.

To properly estimate those contributions, we first analyze the running of the gauge couplings. We match g_R and g_L to the SM strong coupling g_s at the scale $v_\Sigma = 7$ TeV via Eq. (6) and choose $g_R(v_\Sigma) = g_L(v_\Sigma)$. This implies that $g_R(v_\Sigma) = g_L(v_\Sigma) \simeq 1.44$. We then perform the running using the renormalization group equations

$$\frac{\partial g_{R/L}(\mu)}{\partial \log \mu} = -\left(11 - \frac{n_s}{6} - \frac{2n_f}{3}\right)\frac{g^3_{R/L}(\mu)}{16\pi^2}, \quad (24)$$

where n_s is the number of complex scalars and n_f is the number of Dirac fermions in the fundamental representation of the gauge group $\mathrm{SU}(4)_R/\mathrm{SU}(4)_L$ with masses below the scale μ. We find that $g_R(v_R) \simeq 1.01$ and $g_L(v_L) \simeq 1.32$.

(1) *First phase transition*: $\mathrm{SU}(4)_R \to \mathrm{SU}(3)_R$

This transition is triggered when the field $\hat{\Sigma}_R$ develops the VEV as in Eq. (2) with $v_R \approx 5000$ TeV. The relevant background field-dependent masses are

$$m_{X_R}(\phi_R) = \frac{1}{2} g_R \phi_R, \quad m_{Z'_R}(\phi_R) = \frac{M_{Z'_R}}{v_R}\phi_R. \quad (25)$$

The numbers of degrees of freedom corresponding to the gauge bosons X_R and Z'_R are $n_{X_R} = 18$ and $n_{Z'_R} = 3$. The thermal masses are given by

$$\Pi^L_{X_R}(T) = \Pi^L_{Z'_R}(T) = \frac{8}{3} g_R^2 T^2,$$
$$\Pi_\Phi(T) = \Pi_{\chi_{\rm GB}}(T) \approx \frac{1}{8}\left(3g_R^2 + 2\frac{M^2_{Z'_R}}{v_R^2}\right)T^2, \quad (26)$$

where we dropped terms involving the small quartic coupling. The superscript L for the gauge boson thermal masses denotes longitudinal components, Φ is the radial mode, and $\chi_{\rm GB}$ are the Goldstone bosons. The corresponding

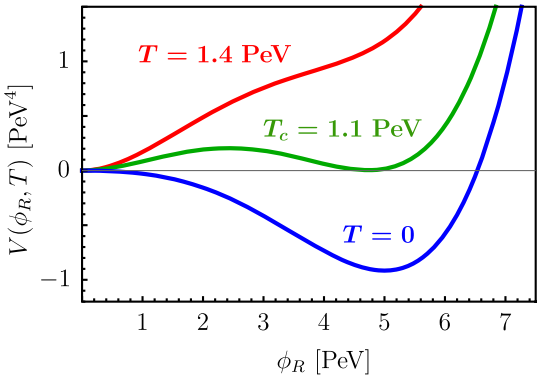

FIG. 1. The effective potential $V_{\rm eff}(\phi_R, T)$ for the temperatures: $T = 0$, $T_c = 1.1$ PeV, and $T = 1.4$ PeV, assuming $v_R = 5$ PeV, $\lambda_R = 0.011$, and after subtracting off the term $V_{\rm eff}(0, T)$.

numbers of degrees of freedom are $n^L_{X_R} = 6$, $n^L_{Z'_R} = 1$, $n_\Phi = 1$, and $n_{\chi_{\rm GB}} = 7$.

Figure 1 shows the full ϕ_R-dependent part of the effective potential, $V_{\rm eff}(\phi_R, T) - V_{\rm eff}(0, T)$, for the parameter values discussed above and for three different temperatures: $T = 0$, $T_c = 1.1$ PeV, and $T = 1.4$ PeV. At the critical temperature T_c the two vacua become degenerate. The order parameter is equal to $\xi^{(R)} \equiv (\phi_R)_c/T_c \approx 4$, indicating a strong first order phase transition.

(2) *Second phase transition*: $\mathrm{SU}(4)_L \to \mathrm{SU}(3)_L$

This transition happens when the field $\hat{\Sigma}_L$ develops the VEV $v_L \approx 40$ TeV. The corresponding background field-dependent masses and thermal masses are obtained from Eqs. (25) and (26) upon substituting $R \to L$. The critical temperature is $T_c \approx 15$ TeV and the order parameter $\xi^{(L)} \approx 3$.

(3) *Third phase transition*: $\mathrm{SU}(3)_R \times \mathrm{SU}(3)_L \to \mathrm{SU}(3)_c$

This symmetry breaking is triggered when $\hat{\Sigma}$ develops the VEV as in Eq. (2) with $v_\Sigma \approx 7$ TeV. For a small z the contribution of the cross terms to the effective potential is small, as are those of the vectorlike fermions Q' and L', even with Yukawas $Y_{ij} \sim 1$ (see, e.g., [65,99] for the corresponding formulas). Therefore, the only relevant background field-dependent mass is that of G'. For transverse components

$$m_{G'}(\phi_\Sigma) = \frac{1}{\sqrt{2}}\sqrt{g_R^2 + g_L^2}\,\phi_\Sigma, \tag{27}$$

with the number of degrees of freedom $n^T_{G'} = 16$. For the longitudinal modes of G' and the SM gluon, the masses $m_i^2(\phi_\Sigma) + \Pi_i^L(T)$ are given by the eigenvalues of the matrix

$$\mathcal{M}_i^2(\phi_\Sigma, T) = \frac{1}{2}\begin{pmatrix} g_R^2(\phi_\Sigma^2 + 4T^2) & -g_R g_L \phi_\Sigma^2 \\ -g_R g_L \phi_\Sigma^2 & g_L^2(\phi_\Sigma^2 + 4T^2) \end{pmatrix}. \tag{28}$$

The numbers of degrees of freedom are $n^L_{G'} = n^L_g = 8$. The thermal masses for the radial modes and Goldstone bosons are

$$\Pi_\Sigma(T) \approx (g_R^2 + g_L^2)T^2 \tag{29}$$

with $n_\Sigma = 32$. A strong first order phase transition occurs since $\xi^{(\Sigma)} \approx 2$ for the critical temperature $T_c \approx 1.7$ TeV.

V. GRAVITATIONAL WAVE SIGNALS

As a result of a first order phase transition, bubbles of true vacuum are nucleated, they expand (with velocity v_w), and eventually they fill up the entire universe. The bubble nucleation rate per unit volume is given by the expression [100]

$$\Gamma(T) \approx \left(\frac{S_3(T)}{2\pi T}\right)^{\frac{3}{2}} T^4 e^{-\frac{S_3(T)}{T}}, \tag{30}$$

where $S_3(T)$ is the Euclidean action

$$S_3(T) = 4\pi \int dr r^2 \left[\frac{1}{2}\left(\frac{d\phi_b}{dr}\right)^2 + V_{\rm eff}(\phi_b, T)\right]. \tag{31}$$

Here $\phi_b(r)$ is the SO(3) symmetric bounce solution describing the profile of the expanding bubble, i.e., the solution of the equation

$$\frac{d^2\phi_b}{dr^2} + \frac{2}{r}\frac{d\phi_b}{dr} - \left.\frac{dV_{\rm eff}(\phi, T)}{d\phi}\right|_{\phi=\phi_b} = 0 \tag{32}$$

with the boundary conditions

$$\left.\frac{d\phi_b}{dr}\right|_{r=0} = 0, \qquad \phi_b(\infty) = \phi_{\rm false}, \tag{33}$$

where $\phi_{\rm false} = 0$ is the field value of the false vacuum.

The phase transition begins at the temperature T_*, called the nucleation temperature, at which $\Gamma(T_*) \approx H^4$, where H is the Hubble value at that time. This is equivalent to

$$\frac{S_3(T_*)}{T_*} \approx 4\log\left(\frac{M_P}{T_*}\right) - \log\left[\left(\frac{4\pi^3 g_*}{45}\right)^2 \left(\frac{2\pi T_*}{S_3(T_*)}\right)^{\frac{3}{2}}\right], \tag{34}$$

where $M_P = 1.22 \times 10^{19}$ GeV is the Planck mass.

Each phase transition continues until most of the universe is filled with bubbles of true vacuum. The inverse of the duration of this process, the so-called $\tilde{\beta}$ parameter, is given by

$$\tilde{\beta} \equiv T_* \frac{d}{dT}\left(\frac{S_3(T)}{T}\right)\bigg|_{T=T_*}. \tag{35}$$

The strength of a phase transition, denoted by α, is defined as

$$\alpha \equiv \frac{\rho_{\rm vac}(T_*)}{\rho_{\rm rad}(T_*)}, \tag{36}$$

where $\rho_{\rm vac}(T_*)$ is the energy density of the false vacuum (i.e., the latent heat released during the phase transition) [101],

$$\rho_{\rm vac}(T_*) = \Delta V_{\rm eff}(T_*) - T_* \left.\frac{\partial \Delta V_{\rm eff}(T)}{\partial T}\right|_{T=T_*} \tag{37}$$

with $\Delta V_{\rm eff}(T) = V_{\rm eff}(\phi_{\rm false}, T) - V_{\rm eff}(\phi_{\rm true}, T)$, and $\rho_{\rm rad}(T_*)$ is the energy density of radiation at nucleation temperature,

$$\rho_{\rm rad}(T_*) = \frac{\pi^2}{30} g_* T_*^4. \tag{38}$$

In the expressions above $\phi_{\rm true}$ is the field value of the true vacuum, whereas g_* is the number of relativistic degrees of freedom at the time of the transition. In our benchmark scenario: $g_*^{(1)} \simeq 274$, $g_*^{(2)} \simeq 252$, and $g_*^{(3)} \simeq 228$. The four parameters α, $\tilde{\beta}$, v_w, and T_* determine the size and peak frequency of the stochastic gravitational wave signal. In our analysis we set the bubble wall velocity to $v_w = 0.6c$ (for an extensive discussion of bubble expansion, see [102,103]).

There are three sources of gravitational waves generated from phase transitions: sound waves, bubble collisions, and magnetohydrodynamic turbulence. Those three contributions combine linearly to give the total gravitational wave signal

$$h^2\Omega_{\rm GW} \approx h^2\Omega_{\rm sound} + h^2\Omega_{\rm collision} + h^2\Omega_{\rm turbulence}. \tag{39}$$

The contribution from sound waves is [103,104]

$$h^2\Omega_{\rm sound}(\nu) \approx (1.86\times 10^{-5}) \frac{v_w}{\tilde{\beta}} \left(\frac{\kappa_s \alpha}{1+\alpha}\right)^2 \left(\frac{100}{g_*}\right)^{\frac{1}{3}} \times \frac{\left(\frac{\nu}{\nu_s}\right)^3}{\left[1 + 0.75\left(\frac{\nu}{\nu_s}\right)^2\right]^{\frac{7}{2}}}, \tag{40}$$

where the model-dependent parameter κ_s is the fraction of the latent heat that is transformed into the bulk motion of the plasma, approximated by [102]

$$\kappa_s \approx \frac{\alpha}{0.73 + 0.083\sqrt{\alpha} + \alpha}, \tag{41}$$

and ν_s is the peak frequency given by

$$\nu_s = (0.019\ {\rm Hz}) \frac{\tilde{\beta}}{v_w} \left(\frac{g_*}{100}\right)^{\frac{1}{6}} \left(\frac{T_*}{100\ {\rm TeV}}\right). \tag{42}$$

The contribution from bubble collisions is [103,105,106]

$$h^2\Omega_{\rm collision}(\nu) \approx (1.66\times 10^{-5}) \frac{1}{\tilde{\beta}^2} \left(\frac{\kappa_c \alpha}{1+\alpha}\right)^2 \left(\frac{100}{g_*}\right)^{\frac{1}{3}} \times \left(\frac{v_w^3}{1 + 2.4 v_w^2}\right) \frac{\left(\frac{\nu}{\nu_c}\right)^{2.8}}{1 + 2.8\left(\frac{\nu}{\nu_c}\right)^{3.8}}, \tag{43}$$

where κ_c is the fraction of the latent heat that is deposited into a thin shell close to the bubble front [107],

$$\kappa_c \approx \frac{0.715\alpha + \frac{4}{27}\sqrt{\frac{3\alpha}{2}}}{1 + 0.715\alpha}, \tag{44}$$

and the peak frequency ν_c is

$$\nu_c = (0.010\ {\rm Hz}) \tilde{\beta} \left(\frac{g_*}{100}\right)^{\frac{1}{6}} \left(\frac{T_*}{100\ {\rm TeV}}\right) \times \left(\frac{1}{1.8 - 0.1 v_w + v_w^2}\right). \tag{45}$$

The contribution from turbulence is [108,109]

$$h^2\Omega_{\rm turbulence}(\nu) \approx (3.35\times 10^{-4}) \frac{v_w}{\tilde{\beta}} \left(\frac{\kappa_t \alpha}{1+\alpha}\right)^{\frac{3}{2}} \left(\frac{100}{g_*}\right)^{\frac{1}{3}} \times \frac{\left(\frac{\nu}{\nu_t}\right)^3}{\left(1 + \frac{8\pi\nu}{h_*}\right)\left(1 + \frac{\nu}{\nu_t}\right)^{\frac{11}{3}}}, \tag{46}$$

where $\kappa_t = \epsilon \kappa_s$ denotes the fraction of the latent heat transformed into magnetohydrodynamic turbulence (following [103], we take $\epsilon = 0.05$), the peak frequency ν_t is

$$\nu_t = (0.027\ {\rm Hz}) \frac{\tilde{\beta}}{v_w} \left(\frac{g_*}{100}\right)^{\frac{1}{6}} \left(\frac{T_*}{100\ {\rm TeV}}\right) \tag{47}$$

and the parameter h_* is [103]

$$h_* = (0.0165\ {\rm Hz}) \left(\frac{g_*}{100}\right)^{\frac{1}{6}} \left(\frac{T_*}{100\ {\rm TeV}}\right). \tag{48}$$

To find the gravitational wave signal from the three phase transitions, we analyzed separately the ϕ_R, ϕ_L, ϕ_Σ-dependent pieces of the potential in Eq. (18). In each case we determined numerically the temperature at which the shape of the potential yields the Euclidean action $S(T_*)$ satisfying Eq. (34). For this nucleation temperature, we calculated the values of the parameters α, $\tilde{\beta}$, and used them to derive the gravitational wave spectrum via Eqs. (39)–(48).

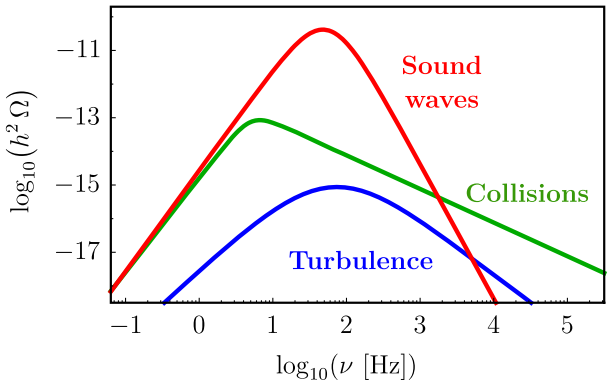

FIG. 2. Contributions to the gravitational wave signal of the phase transition $\mathrm{SU}(4)_R \to \mathrm{SU}(3)_R$ arising from sound waves, bubble collisions, and magnetohydrodynamic turbulence.

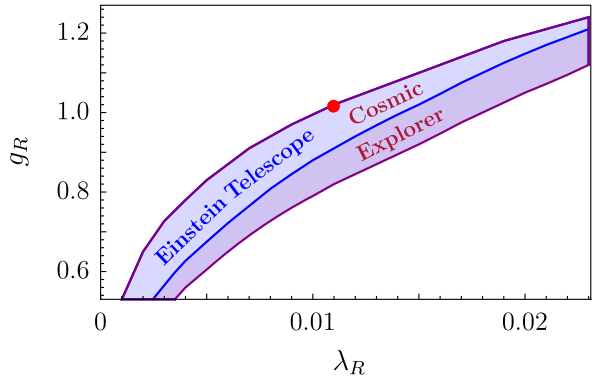

FIG. 3. Regions of parameter space for which a phase transition $\mathrm{SU}(4)_R \to \mathrm{SU}(3)_R$ with $v_R = 5$ PeV gives rise to a gravitational wave signal detectable at the Einstein Telescope (blue) and Cosmic Explorer (blue and purple) with a signal-to-noise ratio greater than five after one year of collecting data (see text for details). The red dot denotes the benchmark parameters adopted in Fig. 4.

Our calculation revealed that in the left-right SU(4) model the sound wave contribution dominates over the contributions from bubble collisions and magnetohydrodynamic turbulence in most of the peak region, thus the shape of the signal is well approximated by Eq. (40) and the peak frequency by Eq. (42). This is illustrated in Fig. 2 for the phase transition associated with $\mathrm{SU}(4)_R \to \mathrm{SU}(3)_R$.

In order to assess how generic are the phase transitions leading to detectable gravitational wave signals in the model, we performed a scan over the relevant parameters. Figure 3 presents the regions of parameter space for the gauge coupling g_R versus the quartic coupling λ_R which yield a first order phase transition $\mathrm{SU}(4)_R \to \mathrm{SU}(3)_R$ (for $v_R = 5$ PeV) giving rise to signals detectable at the Einstein Telescope and Cosmic Explorer, with a signal-to-noise ratio greater than five after one year of collecting data. In particular, the lower boundaries of those regions correspond to the signal-to-noise ratio of five for each experiment. Above the upper boundary, either the value of $S_3(T)/T$ is too large to satisfy the condition in Eq. (34) or the zero temperature vacuum at $v_R \neq 0$ has a higher energy density than the vacuum at $v_R = 0$, which is unphysical, since it would lead to a second transition back to the vacuum with $v_R = 0$. Similarly sized regions of parameter space relevant for the phase transitions $\mathrm{SU}(4)_L \to \mathrm{SU}(3)_L$ (for $v_L = 40$ TeV) and $\mathrm{SU}(3)_R \times \mathrm{SU}(3)_L \to \mathrm{SU}(3)_c$ (for $v_\Sigma = 7$ TeV) yield signals detectable in other gravitational wave experiments.

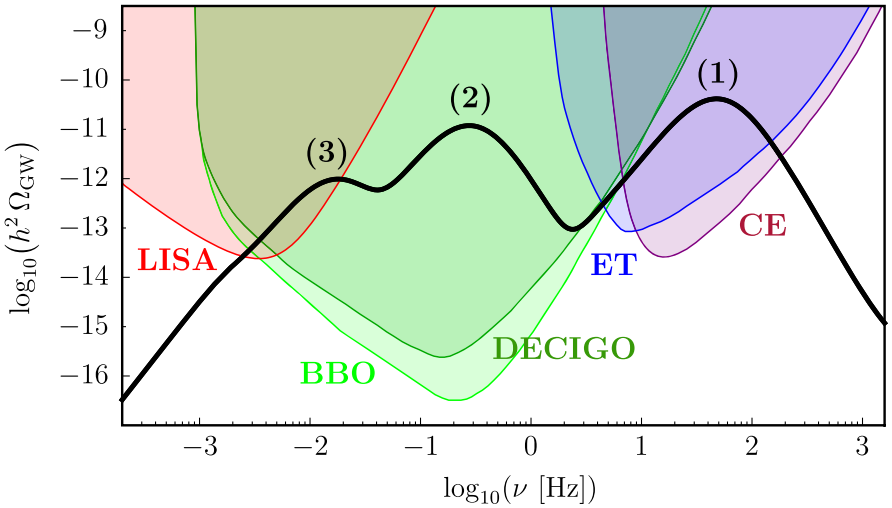

FIG. 4. Gravitational wave signature of the left-right SU(4) model (black line) for the benchmark scenario described in Eq. (16). Overplotted are the sensitivities of the future gravitational wave experiments: LISA in the C1 configuration [103] (red), Big Bang Observer [110] (light green), DECIGO [110] (dark green), Einstein Telescope [111] (blue), and Cosmic Explorer [49] (purple). The three peaks correspond to the phase transitions: (1) $\mathrm{SU}(4)_R \to \mathrm{SU}(3)_R$, (2) $\mathrm{SU}(4)_L \to \mathrm{SU}(3)_L$, and (3) $\mathrm{SU}(3)_R \times \mathrm{SU}(3)_L \to \mathrm{SU}(3)_c$ discussed in Sec. IV.

TABLE II. Values of the parameters α, $\tilde{\beta}$, and T_* for the three phase transitions giving rise to the gravitational wave signal in Fig. 4.

Phase transition	α	$\tilde{\beta}$	T_*
(1) $SU(4)_R \to SU(3)_R$	0.35	270	430 TeV
(2) $SU(4)_L \to SU(3)_L$	0.09	120	6.4 TeV
(3) $SU(3)_R \times SU(3)_L \to SU(3)_c$	0.02	60	0.9 TeV

Figure 4 shows the combined spectrum of gravitational waves from all three phase transitions in our benchmark scenario, with the corresponding parameters summarized in Table II. As expected, each of the phase transitions produces a distinct peak in the spectrum, characterized by a large signal-to-noise ratio. As seen from Eq. (42), the position of individual peaks depends linearly on the nucleation temperature T_*, and thus signals from phase transitions corresponding to higher symmetry breaking scales appear at higher frequencies. The peak frequency depends also linearly on $\tilde{\beta}$. The height of the peak is governed by α and $\tilde{\beta}$; it increases with bigger α and decreases with larger $\tilde{\beta}$. Of course, all those parameters depend on the values of the VEVs, quartic couplings, and gauge couplings in the model.

Within the benchmark scenario, the gravitational wave signal generated by the symmetry breaking $SU(4)_R \to SU(3)_R$ at the scale $v_R \approx 5$ PeV [peak (1)] falls within the sensitivity of the future gravitational wave detectors Cosmic Explorer and Einstein Telescope. The signal resulting from the second phase transition $SU(4)_L \to SU(3)_L$ at the scale $v_L \approx 40$ TeV [peak (2)] is well within the reach of the Big Bang Observer and DECIGO. The third phase transition $SU(3)_R \times SU(3)_L \to SU(3)_c$ occurring at the scale $v_\Sigma \approx 7$ TeV [peak (3)] can also be probed by the Big Bang Observer and DECIGO. In addition, it can be searched for by LISA, but only if the C1 configuration [103] is implemented.

A unique property of the left-right SU(4) model is that the range of peak frequencies for the phase transitions $SU(4)_L \to SU(3)_L$ and $SU(3)_R \times SU(3)_L \to SU(3)_c$ is constrained by the size of the $R_{K^{(*)}}$ anomalies, as described by Eq. (15). In our benchmark scenario we assumed that there is a maximal hierarchy between the scales v_L and v_Σ, which leads to two well-separated peaks in the spectrum. However, if the two scales are comparable, then the size of the flavor anomalies sets the symmetry breaking scale at $v_L \approx v_\Sigma \lesssim 25$ TeV, resulting in a single peak shifted toward lower frequencies compared to peak (2) in Fig. 4. This is still within the reach of the Big Bang Observer and DECIGO.

Finally, we point out that the scale of the symmetry breaking $SU(4)_R \to SU(3)_R$ is not bounded from above. In particular, it can be larger than ∼100 PeV, shifting peak (1) to higher frequencies and escaping the detection at the Cosmic Explorer and Einstein Telescope. A gravitational wave experiment sensitive to such high frequencies would be necessary to probe this scenario.

VI. CONCLUSIONS

Gravitational wave experiments have recently emerged as a powerful tool for testing particle physics models. One class of signatures which those experiments are sensitive to arises from first order phase transitions in the early universe, making them valuable probes of the scalar sector in models with spontaneous symmetry breaking.

In this paper we demonstrated, in the context of the left-right SU(4) model, that gravitational wave detectors can be used to look for signatures specific to the flavor anomalies recently observed at the LHCb, *BABAR*, and Belle experiments. The measured magnitude of lepton universality violation implies that there can be two peaks in the gravitational wave spectrum within the sensitivity of the upcoming LISA, Big Bang Observer, and DECIGO experiments. There is also a possibility of a third peak which could be observed by the Cosmic Explorer and Einstein Telescope.

If the hints of lepton universality violation are confirmed and a gravitational wave signal with features similar to those of the left-right SU(4) model is discovered, this would be a strong motivation for building the 100 TeV collider, which could provide a complementary direct detection method of testing the model.

ACKNOWLEDGMENTS

The author is grateful to Peter Stangl and Yue Zhao for inspiring discussions and helpful comments. This research was supported in part by the U.S. Department of Energy under Award No. DE-SC0009959.

[1] S. L. Glashow, Partial symmetries of weak interactions, Nucl. Phys. **22**, 579 (1961).
[2] S. Weinberg, A Model of Leptons, Phys. Rev. Lett. **19**, 1264 (1967).
[3] A. Salam, Weak and electromagnetic interactions, Conf. Proc. **C680519**, 367 (1968).
[4] H. Fritzsch and M. Gell-Mann, Current Algebra: Quarks and What Else? *Proceedings of the XVI International*

Conference on High Energy Physics (National Accelerator Laboratory, Chicago, 1972), p. 135–165.
[5] H. Fritzsch, M. Gell-Mann, and H. Leutwyler, Advantages of the color octet gluon picture, Phys. Lett. **47B**, 365 (1973).
[6] J. P. Lees *et al.* (*BABAR* Collaboration), Measurement of an excess of $\bar{B} \to D^{(*)}\tau^-\bar{\nu}_\tau$ decays and implications for charged Higgs bosons, Phys. Rev. D **88**, 072012 (2013).
[7] Y. Sato *et al.* (Belle Collaboration), Measurement of the branching ratio of $\bar{B}^0 \to D^{*+}\tau^-\bar{\nu}_\tau$ relative to $\bar{B}^0 \to D^{*+}\ell^-\bar{\nu}_\ell$ decays with a semileptonic tagging method, Phys. Rev. D **94**, 072007 (2016).
[8] R. Aaij *et al.* (LHCb Collaboration), Measurement of the Ratio of the $B^0 \to D^{*-}\tau^+\nu_\tau$ and $B^0 \to D^{*-}\mu^+\nu_\mu$ Branching Fractions Using Three-Prong τ-Lepton Decays, Phys. Rev. Lett. **120**, 171802 (2018).
[9] A. Abdesselam *et al.* (Belle Collaboration), Measurement of $\mathcal{R}(D)$ and $\mathcal{R}(D^*)$ with a semileptonic tagging method, arXiv:1904.08794.
[10] R. Aaij *et al.* (LHCb Collaboration), Test of lepton universality with $B^0 \to K^{*0}\ell^+\ell^-$ decays, J. High Energy Phys. 08 (2017) 055.
[11] A. Abdesselam *et al.* (Belle Collaboration), Test of lepton flavor universality in $B \to K^*\ell^+\ell^-$ decays at Belle, arXiv:1904.02440.
[12] R. Aaij *et al.* (LHCb Collaboration), Test of Lepton Universality Using $B^+ \to K^+\ell^+\ell^-$ Decays, Phys. Rev. Lett. **113**, 151601 (2014).
[13] R. Aaij *et al.* (LHCb Collaboration), Search for Lepton-Universality Violation in $B^+ \to K^+\ell^+\ell^-$ Decays, Phys. Rev. Lett. **122**, 191801 (2019).
[14] N. Kosnik, Model independent constraints on leptoquarks from $b \to s\ell^+\ell^-$ processes, Phys. Rev. D **86**, 055004 (2012).
[15] R. Alonso, B. Grinstein, and J. M. Camalich, $SU(2) \times U(1)$ Gauge Invariance and the Shape of New Physics in Rare B Decays, Phys. Rev. Lett. **113**, 241802 (2014).
[16] B. Bhattacharya, A. Datta, D. London, and S. Shivashankara, Simultaneous explanation of the R_K and $R(D^{(*)})$ puzzles, Phys. Lett. B **742**, 370 (2015).
[17] R. Alonso, B. Grinstein, and J. M. Camalich, Lepton universality violation and lepton flavor conservation in B-meson decays, J. High Energy Phys. 10 (2015) 184.
[18] B. Bhattacharya, A. Datta, J.-P. Guevin, D. London, and R. Watanabe, Simultaneous explanation of the R_K and $R_{D^{(*)}}$ puzzles: A model analysis, J. High Energy Phys. 01 (2017) 015.
[19] L.-S. Geng, B. Grinstein, S. Jager, J. M. Camalich, X.-L. Ren, and R.-X. Shi, Towards the discovery of new physics with lepton-universality ratios of $b \to s\ell\ell$ decays, Phys. Rev. D **96**, 093006 (2017).
[20] A. K. Alok, J. Kumar, D. Kumar, and R. Sharma, Lepton flavor non-universality in the B-sector: A global analyses of various new physics models, Eur. Phys. J. C **79**, 707 (2019).
[21] D. Buttazzo, A. Greljo, G. Isidori, and D. Marzocca, B-physics anomalies: A guide to combined explanations, J. High Energy Phys. 11 (2017) 044.
[22] J. Kumar, D. London, and R. Watanabe, Combined explanations of the $b \to s\mu^+\mu^-$ and $b \to c\tau^-\bar{\nu}$ anomalies: A general model analysis, Phys. Rev. D **99**, 015007 (2019).
[23] N. Assad, B. Fornal, and B. Grinstein, Baryon number and lepton universality violation in leptoquark and diquark models, Phys. Lett. B **777**, 324 (2018).
[24] L. Calibbi, A. Crivellin, and T. Li, A model of vector leptoquarks in view of the B-physics anomalies, Phys. Rev. D **98**, 115002 (2018).
[25] L. Di Luzio, A. Greljo, and M. Nardecchia, Gauge leptoquark as the origin of B-physics anomalies, Phys. Rev. D **96**, 115011 (2017).
[26] M. Bordone, C. Cornella, J. Fuentes-Martin, and G. Isidori, A three-site gauge model for flavor hierarchies and flavor anomalies, Phys. Lett. B **779**, 317 (2018).
[27] R. Barbieri and A. Tesi, B-decay anomalies in Pati-Salam SU(4), Eur. Phys. J. C **78**, 193 (2018).
[28] M. Blanke and A. Crivellin, B Meson Anomalies in a Pati-Salam Model within the Randall-Sundrum Background, Phys. Rev. Lett. **121**, 011801 (2018).
[29] A. Greljo and B. A. Stefanek, Third family quark-lepton unification at the TeV scale, Phys. Lett. B **782**, 131 (2018).
[30] L. Di Luzio, J. Fuentes-Martin, A. Greljo, M. Nardecchia, and S. Renner, Maximal flavour violation: A Cabibbo mechanism for leptoquarks, J. High Energy Phys. 11 (2018) 081.
[31] J. Fuentes-Martin, M. Reig, and A. Vicente, Strong CP problem with low-energy emergent QCD: The 4321 case, Phys. Rev. D **100**, 115028 (2019).
[32] J. Fuentes-Martin and P. Stangl, Third-family quark-lepton unification with a fundamental composite Higgs, Phys. Lett. B **811**, 135953 (2020).
[33] D. Guadagnoli, M. Reboud, and P. Stangl, The dark side of 4321, J. High Energy Phys. 10 (2020) 084.
[34] S. Balaji, R. Foot, and M. A. Schmidt, Chiral SU(4) explanation of the $b \to s$ anomalies, Phys. Rev. D **99**, 015029 (2019).
[35] B. Fornal, S. A. Gadam, and B. Grinstein, Left-right SU(4) vector leptoquark model for flavor anomalies, Phys. Rev. D **99**, 055025 (2019).
[36] J. M. Cline, J. M. Cornell, D. London, and R. Watanabe, Hidden sector explanation of B-decay and cosmic ray anomalies, Phys. Rev. D **95**, 095015 (2017).
[37] D. Marzocca, Addressing the B-physics anomalies in a fundamental composite Higgs model, J. High Energy Phys. 07 (2018) 121.
[38] D. Guadagnoli, M. Reboud, and O. Sumensari, A gauged horizontal $SU(2)$ symmetry and $R_{K^{(*)}}$, J. High Energy Phys. 11 (2018) 163.
[39] S.-P. Li, X.-Q. Li, Y.-D. Yang, and X. Zhang, $R_{D^{(*)}}$, $R_{K^{(*)}}$ and neutrino mass in the 2HDM-III with right-handed neutrinos, J. High Energy Phys. 09 (2018) 149.
[40] T. Faber, M. Hudec, M. Malinsky, P. Meinzinger, W. Porod, and F. Staub, A unified leptoquark model confronted with lepton non-universality in B-meson decays, Phys. Lett. B **787**, 159 (2018).
[41] B. Allanach and J. Davighi, Third family hypercharge model for $R_{K^{(*)}}$ and aspects of the fermion mass problem, J. High Energy Phys. 12 (**2018**) 075.

[42] Y. Cai, J. Gargalionis, M. A. Schmidt, and R. R. Volkas, Reconsidering the one leptoquark solution: Flavor anomalies and neutrino mass, J. High Energy Phys. 10 (2017) 047.

[43] J. Heeck and D. Teresi, Pati-Salam explanations of the B-meson anomalies, J. High Energy Phys. 12 (2018) 103.

[44] D. Becirevic, I. Dorsner, S. Fajfer, D. A. Faroughy, N. Kosnik, and O. Sumensari, Scalar leptoquarks from GUT to accommodate the B-physics anomalies, Phys. Rev. D **98**, 055003 (2018).

[45] I. Bigaran, J. Gargalionis, and R. R. Volkas, A near-minimal leptoquark model for reconciling flavour anomalies and generating radiative neutrino masses, J. High Energy Phys. 10 (2019) 106.

[46] J. Aasi *et al.* (LIGO Scientific Collaboration), Advanced LIGO, Classical Quantum Gravity **32**, 074001 (2015).

[47] F. Acernese *et al.* (Virgo Collaboration), Advanced Virgo: A second-generation interferometric gravitational wave detector, Classical Quantum Gravity **32**, 024001 (2015).

[48] P. Amaro-Seoane *et al.* (LISA Collaboration), Laser interferometer space antenna, arXiv:1702.00786.

[49] D. Reitze *et al.*, Cosmic Explorer: The U.S. contribution to gravitational-wave astronomy beyond LIGO, Bull. Am. Astron. Soc. **51**, 035 (2019), https://baas.aas.org/pub/2020n7i035/release/1.

[50] M. Punturo *et al.*, The Einstein Telescope: A third-generation gravitational wave observatory, Classical Quantum Gravity **27**, 194002 (2010).

[51] S. Kawamura *et al.*, The Japanese space gravitational wave antenna: DECIGO, Classical Quantum Gravity **28**, 094011 (2011).

[52] J. Crowder and N. J. Cornish, Beyond LISA: Exploring future gravitational wave missions, Phys. Rev. D **72**, 083005 (2005).

[53] R. Apreda, M. Maggiore, A. Nicolis, and A. Riotto, Gravitational waves from electroweak phase transitions, Nucl. Phys. **B631**, 342 (2002).

[54] C. Grojean and G. Servant, Gravitational waves from phase transitions at the electroweak scale and beyond, Phys. Rev. D **75**, 043507 (2007).

[55] L. Leitao, A. Megevand, and A. D. Sanchez, Gravitational waves from the electroweak phase transition, J. Cosmol. Astropart. Phys. 10 (2012) 024.

[56] P. Schwaller, Gravitational Waves from a Dark Phase Transition, Phys. Rev. Lett. **115**, 181101 (2015).

[57] F. P. Huang and X. Zhang, Probing the gauge symmetry breaking of the Early Universe in 3-3-1 models and beyond by gravitational waves, Phys. Lett. B **788**, 288 (2019).

[58] F. P. Huang and J.-H. Yu, Exploring inert dark matter blind spots with gravitational wave signatures, Phys. Rev. D **98**, 095022 (2018).

[59] S. V. Demidov, D. S. Gorbunov, and D. V. Kirpichnikov, Gravitational waves from phase transition in split NMSSM, Phys. Lett. B **779**, 191 (2018).

[60] K. Hashino, M. Kakizaki, S. Kanemura, P. Ko, and T. Matsui, Gravitational waves from first order electroweak phase transition in models with the $\mathrm{U}(1)_X$ gauge symmetry, J. High Energy Phys. 06 (2018) 088.

[61] E. Madge and P. Schwaller, Leptophilic dark matter from gauged lepton number: Phenomenology and gravitational wave signatures, J. High Energy Phys. 02 (2019) 048.

[62] A. Ahriche, K. Hashino, S. Kanemura, and S. Nasri, Gravitational waves from phase transitions in models with charged singlets, Phys. Lett. B **789**, 119 (2019).

[63] V. Brdar, A. J. Helmboldt, and J. Kubo, Gravitational waves from first-order phase transitions: LIGO as a window to unexplored seesaw scales, J. Cosmol. Astropart. Phys. 02 (2019) 021.

[64] D. Croon, T. E. Gonzalo, and G. White, Gravitational waves from a Pati-Salam phase transition, J. High Energy Phys. 02 (2019) 083.

[65] A. Angelescu and P. Huang, Multistep strongly first order phase transitions from new fermions at the TeV scale, Phys. Rev. D **99**, 055023 (2019).

[66] T. Hasegawa, N. Okada, and O. Seto, Gravitational waves from the minimal gauged $U(1)_{B-L}$ model, Phys. Rev. D **99**, 095039 (2019).

[67] P. S. B. Dev, F. Ferrer, Y. Zhang, and Y. Zhang, Gravitational waves from first-order phase transition in a simple axion-like particle model, J. Cosmol. Astropart. Phys. 11 (2019) 006.

[68] V. Brdar, L. Graf, A. J. Helmboldt, and X.-J. Xu, Gravitational waves as a probe of left-right symmetry breaking, J. Cosmol. Astropart. Phys. 12 (2019) 027.

[69] X. Wang, F. P. Huang, and X. Zhang, Gravitational wave and collider signals in complex two-Higgs doublet model with dynamical CP-violation at finite temperature, Phys. Rev. D **101**, 015015 (2020).

[70] A. Greljo, T. Opferkuch, and B. A. Stefanek, Gravitational Imprints of Flavor Hierarchies, Phys. Rev. Lett. **124**, 171802 (2020).

[71] B. Von Harling, A. Pomarol, O. Pujolàs, and F. Rompineve, Peccei-Quinn phase transition at LIGO, J. High Energy Phys. 04 (2020) 195.

[72] E. Hall, T. Konstandin, R. McGehee, H. Murayama, and G. Servant, Baryogenesis from a dark first-order phase transition, J. High Energy Phys. 04 (2020) 042.

[73] W.-C. Huang, F. Sannino, and Z.-W. Wang, Gravitational waves from Pati-Salam dynamics, Phys. Rev. D **102**, 095025 (2020).

[74] D. I. Britton *et al.*, Measurement of the $\pi^+ \to e^+\nu$ Branching Ratio, Phys. Rev. Lett. **68**, 3000 (1992).

[75] D. I. Britton *et al.*, Measurement of the $\pi^+ \to e^+\nu$ branching ratio, Phys. Rev. D **49**, 28 (1994).

[76] G. Czapek *et al.*, Branching Ratio for the Rare Pion Decay into Positron and Neutrino, Phys. Rev. Lett. **70**, 17 (1993).

[77] D. Ambrose *et al.* (BNL E871 Collaboration), First Observation of the Rare Decay Mode $K_L^0 \to e^+e^-$, Phys. Rev. Lett. **81**, 4309 (1998).

[78] D. Ambrose *et al.* (BNL Collaboration), New Limit on Muon and Electron Lepton Number Violation from $K_L^0 \to \mu^\pm e^\mp$ Decay, Phys. Rev. Lett. **81**, 5734 (1998).

[79] D. Ambrose *et al.* (E871 Collaboration), Improved Branching Ratio Measurement for the Decay $K_L^0 \to \mu^+\mu^-$, Phys. Rev. Lett. **84**, 1389 (2000).

[80] R. Appel *et al.*, Search for Lepton Flavor Violation in K^+ Decays, Phys. Rev. Lett. **85**, 2877 (2000).

[81] A. Sher *et al.*, An improved upper limit on the decay $K^+ \to \pi^+\mu^+e^-$, Phys. Rev. D **72**, 012005 (2005).

[82] F. Ambrosino *et al.* (KLOE Collaboration), Precise measurement of $\Gamma(K \to e\nu(\gamma))/\Gamma(K \to \mu\nu(\gamma))$ and study of

$K \to e\nu\gamma$, Eur. Phys. J. C **64**, 627 (2009); Erratum, Eur. Phys. J. C **65**, 703 (2010).
[83] B. Aubert *et al.* (*BABAR* Collaboration), Measurements of branching fractions, rate asymmetries, and angular distributions in the rare decays $B \to K\ell^+\ell^-$ and $B \to K^*\ell^+\ell^-$, Phys. Rev. D **73**, 092001 (2006).
[84] B. Aubert *et al.* (*BABAR* Collaboration), Search for the Rare Decay $B \to \pi l^+ l^-$, Phys. Rev. Lett. **99**, 051801 (2007).
[85] B. Aubert *et al.* (*BABAR* Collaboration), Search for the Decay $B^+ \to K^+\tau^\mp\mu^\pm$, Phys. Rev. Lett. **99**, 201801 (2007).
[86] B. Aubert *et al.* (*BABAR* Collaboration), Searches for the decays $B^0 \to \ell^\pm\tau^\mp$ and $B^+ \to \ell^+\nu$ (l = e, μ) using hadronic tag reconstruction, Phys. Rev. D **77**, 091104 (2008).
[87] T. Aaltonen *et al.* (CDF Collaboration), Search for the Decays $B_s^0 \to e^+\mu^-$ and $B_s^0 \to e^+e^-$ in CDF Run II, Phys. Rev. Lett. **102**, 201801 (2009).
[88] R. Aaij *et al.* (LHCb Collaboration), Search for the lepton-flavour violating decays $B_s^0 \to e^\pm\mu^\mp$, J. High Energy Phys. 03 (2018) 078.
[89] R. Aaij *et al.* (LHCb Collaboration), Measurement of the $B_s^0 \to \mu^+\mu^-$ Branching Fraction and Effective Lifetime and Search for $B^0 \to \mu^+\mu^-$ Decays, Phys. Rev. Lett. **118**, 191801 (2017).
[90] R. Aaij *et al.* (LHCb Collaboration), Search for the Decays $B_s^0 \to \tau^+\tau^-$ and $B^0 \to \tau^+\tau^-$, Phys. Rev. Lett. **118**, 251802 (2017).
[91] B. Aubert *et al.* (*BABAR* Collaboration), Search for Lepton Flavor Violating Decays $\tau^\pm \to \ell^\pm\pi^0$, $\ell^\pm\eta$, $\ell^\pm\eta'$, Phys. Rev. Lett. **98**, 061803 (2007).
[92] Y. Miyazaki *et al.* (Belle Collaboration), Search for lepton flavor violating τ^- decays into $\ell^-\eta$, $\ell^-\eta'$ and $\ell^-\pi^0$, Phys. Lett. B **648**, 341 (2007).
[93] Y. Miyazaki *et al.* (Belle Collaboration), Search for lepton flavor violating τ^- decays into $\ell^- K_s^0$ and $\ell^- K_s^0 K_s^0$, Phys. Lett. B **692**, 4 (2010).
[94] W. H. Bertl *et al.* (SINDRUM II Collaboration), A search for muon to electron conversion in muonic gold, Eur. Phys. J. C **47**, 337 (2006).
[95] A. M. Sirunyan *et al.* (CMS Collaboration), Search for High mass Dijet resonances with a new background prediction method in proton-proton collisions at $\sqrt{s} =$ 13 TeV, J. High Energy Phys. 05 (2020) 033.
[96] G. W. Anderson and L. J. Hall, Electroweak phase transition and baryogenesis, Phys. Rev. D **45**, 2685 (1992).
[97] M. Quiros, Field theory at finite temperature and phase transitions, Acta Phys. Pol. B **38**, 3661 (2007), https://www.actaphys.uj.edu.pl/fulltext?series=Reg&vol=38&page=3661.
[98] D. Comelli and J. R. Espinosa, Bosonic Thermal masses in supersymmetry, Phys. Rev. D **55**, 6253 (1997).
[99] H. Davoudiasl, I. Lewis, and E. Ponton, Electroweak phase transition, Higgs diphoton rate, and new heavy fermions, Phys. Rev. D **87**, 093001 (2013).
[100] A. D. Linde, Decay of the false vacuum at finite temperature, Nucl. Phys. **B216**, 421 (1983).
[101] J. Ellis, M. Lewicki, and J. M. No, On the maximal strength of a first-order electroweak phase transition and its gravitational wave signal, J. Cosmol. Astropart. Phys. 04 (2019) 003.
[102] J. R. Espinosa, T. Konstandin, J. M. No, and G. Servant, Energy budget of cosmological first-order phase transitions, J. Cosmol. Astropart. Phys. 06 (2010) 028.
[103] C. Caprini *et al.*, Science with the space-based interferometer eLISA. II: Gravitational waves from cosmological phase transitions, J. Cosmol. Astropart. Phys. 04 (2016) 001.
[104] M. Hindmarsh, S. J. Huber, K. Rummukainen, and D. J. Weir, Gravitational Waves from the Sound of a First Order Phase Transition, Phys. Rev. Lett. **112**, 041301 (2014).
[105] A. Kosowsky, M. S. Turner, and R. Watkins, Gravitational radiation from colliding vacuum bubbles, Phys. Rev. D **45**, 4514 (1992).
[106] S. J. Huber and T. Konstandin, Gravitational wave production by collisions: More bubbles, J. Cosmol. Astropart. Phys. 09 (2008) 022.
[107] M. Kamionkowski, A. Kosowsky, and M. S. Turner, Gravitational radiation from first order phase transitions, Phys. Rev. D **49**, 2837 (1994).
[108] C. Caprini and R. Durrer, Gravitational waves from stochastic relativistic sources: Primordial turbulence and magnetic fields, Phys. Rev. D **74**, 063521 (2006).
[109] C. Caprini, R. Durrer, and G. Servant, The stochastic gravitational wave background from turbulence and magnetic fields generated by a first-order phase transition, J. Cosmol. Astropart. Phys. 12 (2009) 024.
[110] K. Yagi and N. Seto, Detector configuration of DECIGO/BBO and identification of cosmological neutron-star binaries, Phys. Rev. D **83**, 044011 (2011); Erratum, Phys. Rev. D **95**, 109901 (2017).
[111] B. Sathyaprakash *et al.*, Scientific objectives of Einstein Telescope, Classical Quantum Gravity **29**, 124013 (2012); Erratum, Classical Quantum Gravity **30**, 079501 (2013).